

Numerical Simulation of Metal Thermal Spraying

J. Anagnostopoulos, D. Bouris, K. Nikas and G. Bergeles

Laboratory of Aerodynamics, Mechanical Engineering Department, National Technical University of Athens, 15770, Athens, Greece, e-mail: bergeles@fluid.mech.ntua.gr

Abstract

The objective of this work is the investigation of the effect of the geometric and operating parameters of the metal thermal spraying process on the mechanical-tribological properties of the resulting coatings, in order to produce coatings with the optimum behaviour in friction-damage conditions. This is achieved by the numerical simulation of the physical mechanisms involved in the coating production process and the conduction of numerical experiments. A two-phase particle laden Reynolds averaged flow solver is used for the thermal spraying process. The tune-up and the reliability checks of the computational code are accomplished with the reference to industrial experimental measurements in laboratory and semi-industrial arrangements. Moreover, the influence of several parameters, which determine the final quality of the coating, such as the metal particle size, the temperature, and the particles velocity distribution on impingement are numerically examined.

1. Introduction

The process of metal coating production using metal powder in metal thermal spraying involves several complicated physical mechanisms. In some cases i.e in which use of electrical arc is made for the heating up of the carrier gas to plasma state but in ambient pressure, the flow conditions are such that the fluid can be assumed as incompressible; however in cases of plasma spraying under vacuum conditions the flow can be even supersonic, as is the case of high-speed spraying of oxygen-fuel jet, in which multiple shock waves occur downstream of the nozzle.

The high plasma temperature and its intense variation within the flow field and especially in the mixing area of the jet have to be taken into account particularly in calculating the properties of both the gas and the metal particles carried by the gas phase. The electrical arc is usually not modeled. However, its efficiency, i.e. its heat input to the plasma flow, is evaluated from measurements and it is considered known. The calculations of heat transfer to the particles are critical for their final state when they impinge on the surface to be coated. When the thermal conductivity of the powder material is much larger of that of the plasma, the particles' temperature could be assumed as constant [1]. The heat transfer due to the plasma ionization, i.e. the particles' electrical charge, is usually negligible compared to the convection heat transfer, and becomes important only in cases with high plasma temperatures and large particles [2].

For the particulate phase, the Lagrangian approach is followed, as it makes easier the incorporation into the particle motion external forces other than the aerodynamic resistance (e.g. Basset, thermophoresis, electrostatic etc.). Depending on the spraying conditions, the effects of some of the above forces could be very important [3]. Moreover,

the interaction between the particles and the particles-gas phase might also be important in some specific spraying cases, like the plasma jet in vacuum conditions.

The basic parameters affecting the coatings' quality are the duration of the particles deformation during impact and their final diameter after the solidification. These characteristics depend on the physical properties of the powder material (density, elasticity, surface tension etc.), as well as the impact conditions (impact velocity and temperatures of the particles and the substrate). This complex dependence can be evaluated with the aid of semi-empirical approaches [1, 4], which proved to be reliable compared to corresponding analytical models [5, 6].

The methodology used for the simulation of the above mechanisms involved in thermal plasma spraying in ambient pressure is described in this study. The final target of this effort is the capability of predicting the coating quality and improvement of the spraying conditions.

2. Numerical Simulation

The numerical simulation of the thermal spraying of metal powder was based on a two-phase flow computational code which has been successfully used in the Aerodynamics Laboratory of NTUA for gas-droplets and gas-particles flows [7, 8]. Only the basic characteristics of the code are mentioned here, as the control volume technique for the solution of the continuous phase, the SIMPLE method, k- ϵ turbulence model, and a stochastic Lagrangian particle tracking technique, which calculates representative particle trajectories to produce correct statistical results for the properties of the particulate phase in the computational domain are considered standard [7, 8].

The simulation of the mixing of the Argon (Ar)-jet flow with the ambient air was done by solving extra equations for the concentration of the gas plasma and an enthalpy conservation equation; they both have the following general form (polar coordinates, x, r, θ):

$$\frac{\partial(\rho u \Phi)}{\partial x} + \frac{\partial(r \rho v \Phi)}{r \partial r} + \frac{\partial(r \rho w \Phi)}{r \partial \theta} = \frac{\partial}{\partial x}(\Gamma_{\Phi} \frac{\partial \Phi}{\partial x}) + \frac{\partial}{\partial r}(r \Gamma_{\Phi} \frac{\partial \Phi}{\partial r}) + \frac{\partial}{\partial \theta}(\Gamma_{\Phi} \frac{\partial \Phi}{\partial \theta}) + S_{\Phi} + S_{p,\Phi} \quad (1)$$

where Φ is the Argon concentration or the mixture enthalpy; all equations governing the two-phase flow field have the same general form as the (1) above, where Γ_{Φ} the coefficient of turbulent diffusion and S_{Φ} , $S_{p,\Phi}$ the corresponding source terms of the gaseous and particulate phases [7, 8].

The calculation of the Argon-air mixture properties (density, specific heat, viscosity) is based on the local concentration of each component as a function of temperature:

$$T = h / \sum_j (m_j \overline{C_{p,j}}) \quad (2)$$

where h is the enthalpy and m_j , $\overline{C_{p,j}}$ are the concentration and the specific heat of the component j .

The calculation of the particle temperature at every time-step during the simulation of the particle trajectory is based on the calculation of the heat transfer rate with the gaseous phase as well as the rate of (possible) particle evaporation:

$$C_p \frac{dT_p}{dt} = Q_c + \frac{L}{m_p} \frac{dm_p}{dt} \quad (3)$$

where m_p , T_p and C_p are the mass, the temperature and the particle's specific heat, L is the latent heat of evaporation and Q_c is the convection heat transfer rate.

The source terms of the particulate phase are added to the continuity and enthalpy equations in order to take into account the mass and energy exchange between the two phases. Moreover, the equation of the aerodynamic resistance of a particle has been modified in order to take account for the effects due to the significant variation of the fluid properties (density, viscosity) in the boundary layer of the particle [9].

The possible effect of the other forces in the particle motion was investigated for the metal thermal spraying conditions examined here (see also [3, 9]): The Basset forces are very small compared to the aerodynamic resistance ($d_p < 100 \mu m$). The thermophoretic forces are negligible close to the nozzle, because the relative velocity of the particles-gas is large there and very small far away from the nozzle due to the decreased temperature gradients. The electrostatic forces, which could be developed due to the electric charge of particles, are unimportant compared to the aerodynamic resistance, even inside the electrical arc. Finally, the particle gravity and buoyancy forces have practically zero effect as verified by numerical results.

The prediction of the pattern and the quality of the sprayed surface, which is the main scope of this work, has been realised by developing a simple methodology based on theoretical and experimental-empirical data provided by the literature [3, 4] and on special measurements provided by the industry (CERECO).

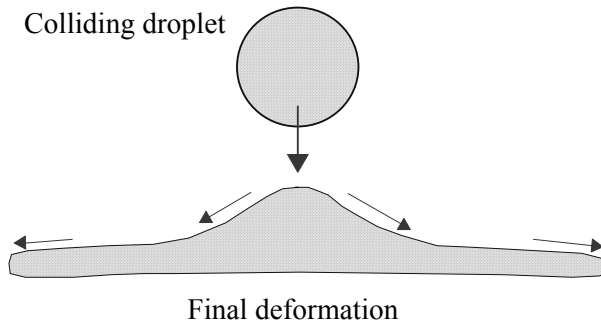


Figure 1. Droplet behaviour during the impact.

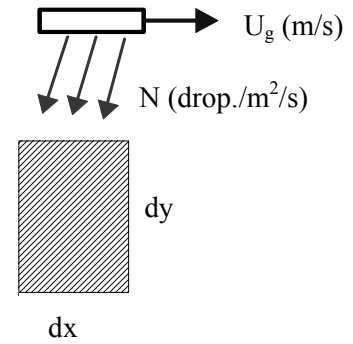


Figure 2. Definition of the covered surface fraction

A hot powder droplet which impacts on a surface is deformed and spreads on the surface while at the same moment it is cooled down and finally solidified (Figure 1). The fast solidification on the interface between the droplet and the material may result in the development of micro pores, whereas larger pores can be caused during the impact and spreading of a droplet on a rough and solid substrate, during the rising of the material due to the impact of liquefied particles or due to the particle impingement onto a liquid substrate.

The porosity of the coating is the basic quality criterion of the surface, while the efficiency criterion of the spraying process is characterized by the amount of the very expensive-powder losses. Powder loss can be arisen due to the insufficient impact on a relatively cool and rough substrate or due to material ejection during the impact process.

A new computational quantity, the covered surface fraction, P_c , is introduced, which is equal to the proportion of the surface occupied by the powder particles, after one sweep of the spraying gun (Figure 2).

$$P_c = N_i dx \left(\pi D_{s,i}^2 / 4 \right) / U_g \quad (4)$$

where N_i is the number of particles of size i which collide per unit surface and time and $D_{s,i}$ is the final diameter of these particles and U_g is the gun traverse speed. The particle number,

N_i , the final diameter, the impact velocity and temperature of the particles can be numerically calculated by the present numerical procedure, whilst the final particle diameter $D_{s,i}$, after solidification, is taken from semi-empirical approaches [1, 4].

According to the above and neglecting the micro pores, the coating porosity V_p , i.e. the volume of the cavities developed on the final surface can be assumed as proportional to the percentage of the covered surface being either in a solidified or a liquefied condition:

$$V_p = a_0 + a_1 P_c \quad (5)$$

On the other hand, the powder loss is not favored in high values of P_c , as high values preserve a warmer and smoother substrate. Therefore, as a first approximation, the thermal spraying efficiency (powder usage) η_α can be written as:

$$\eta_\alpha = b_0 + b_1 P_c \quad (6)$$

The coefficients appearing in the previous equations (5) and (6), related mainly to the material of the powder and the geometry of the spraying gun, can be calibrated for certain spraying conditions as in the case experimentally investigated by CERECO, and described in the following sections.

3. Results

The results which are presented here have been obtained using a very large number of particles injected into the flow field so as statistically independent results are achieved for both, gas and solid phases [7]. The numerical grids were dense enough to secure grid independent results. A locally refined grid [10] was imposed in the area of the nozzle (Figure 4), in order to improve the accuracy of the results there, without significantly increasing the computational demands.

3.1 Reliability test for the two-phase code

The developed algorithm was first tested in the prediction of the two-phase flow field in a laboratory experimental configuration of metal spraying of Argon in air for several spraying conditions (Figure 3) as it is reported in [9] and outlined in Table 1.

Table 1. Spraying conditions by Lee (1984).

Case	Power (V)	Strength (A)	Arc efficiency (%)	Primary flow (Nm ³ /h)	Secondary flow (Nm ³ /h)
1	17.9	367	23	0.9	0.474
2	17.3	375	21	0.708	0.474
3	17.3	375	18.7	0.708	0.368
4	16.9	375	16.5	0.524	0.368
5	18.3	315	26.4	0.9	0.59
6	16.6	330	20	0.623	0.474

The spherical and neutrally charged particles of Al_2O_3 have a size of 5-15 μm and enter into the main flow at ambient temperature by the secondary stream, 4 mm upstream of the nozzle inlet which has a diameter of 8 mm. A non-uniform grid of 40x40 nodes with additional local refinement of 45x45 nodes in the nozzle area (axisymmetric flow and corrections due to the jet slope, [9]) have been used for the solution.

The statistical results for the radial velocity distribution of the injected particles (150000 paths) are compared in Figure 5 with the corresponding measurements [9] at two

different distances from the nozzle exit. The agreement is satisfactory in all cases verifying the reliability of the code.

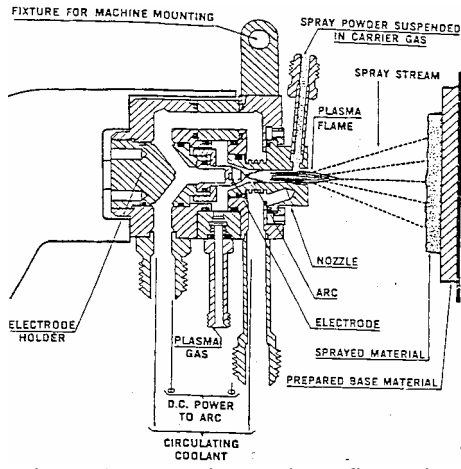


Figure 3. Experimental configuration of metal thermal spraying.

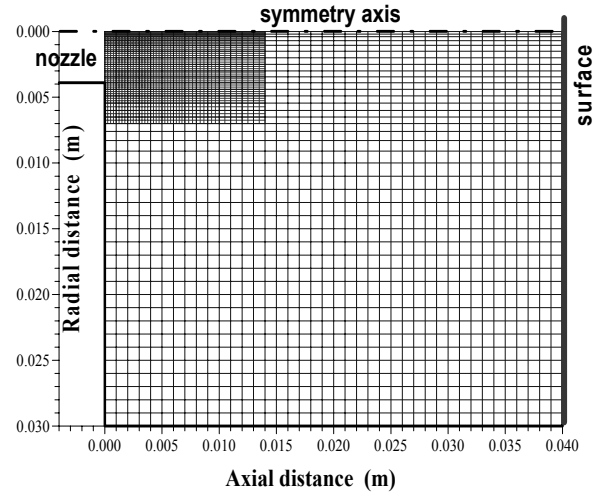


Figure 4. Computational grid.

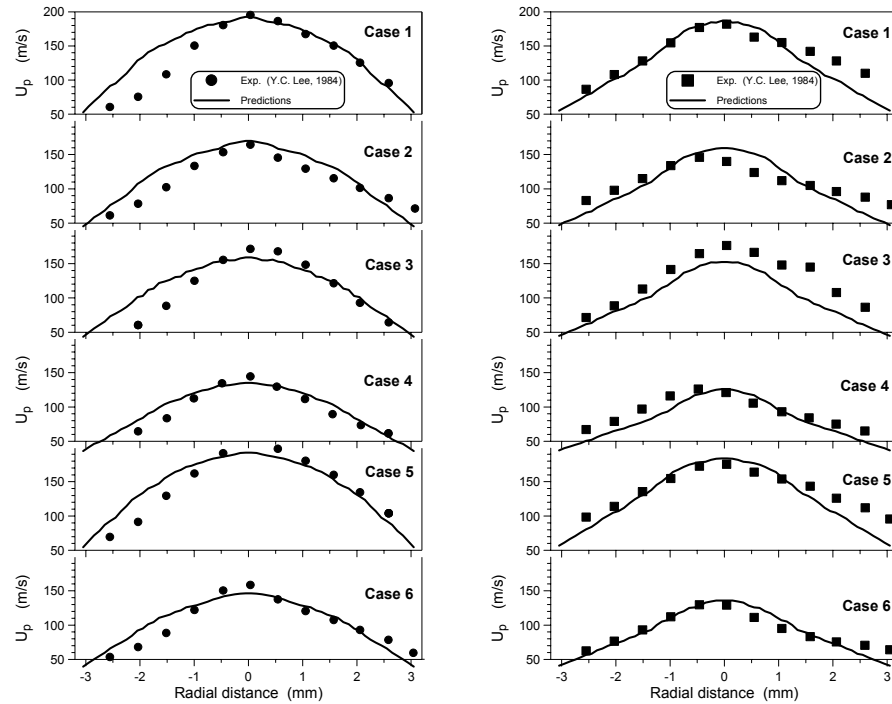


Figure 5. Particle radial velocity in distance: a) 2.54 mm, and b) 6.35 mm.

3.2 Simulation of thermal metal spraying with the CERECO configuration

The next part of this study is concerned with the simulation of the industrial apparatus of thermal plasma spraying of CERECO having a similar gun geometry to that of Figure 3, but with different operating conditions, as outlined in Table 2.

For the exact simulation of this geometry the computational grid has been extended upstream of the nozzle, in order to accommodate the plasma spraying position (radial spraying, Figure 3). Since, a three-dimensional flow field arises, a main grid of 64x42x11 nodes and a local grid refinement of 48x38x11 nodes have been used. Figure 6

shows contours of constant gas axial velocity and temperature on a vertical plane, which passes through the powder nozzle axis. Due to the radial injection of the particles and carrier gas, the jet diverges by an angle of 6 degrees from the nozzle axis. This divergence increases as the particles' diameter becomes bigger and reaches the value of 16° for the biggest ones. This has an effect on the temperature of the particles, which is lower as the large particles diverge more from the hot core of the jet. Moreover, the impact on the surface is not perpendicular but at an angle which decreases as the particles' diameter increases (from 78° for the smallest to 71° for the largest).

The heat transfer rate is higher for the smallest particles. Therefore the small particles increase initially their temperature, but they cool also faster; therefore all particles arrive on the surface with about the same temperature (2200-2300 K, more than 1000 K higher than the gas temperature). The mean particle impact velocity is 100-200 m/s; smaller for the biggest particles, which due to their increased inertia cannot adjust to the gas velocity. Indicative impact particle velocity and temperature distributions are shown in Figure 7 for particles of 27.5 μm diameter.

Table 2. Metal thermal Spraying conditions CERECO.

Nozzle diameter	10.5 mm	Voltage	900 A
Spraying distance	100 mm	Intensity	70 V
Primary gas, flowrate	Ar, 120 l/min	Powder, material	WC/12%Co
Secondary gas, flowrate	He, 20 l/min	Flowrate	25 g/min
Carrier powder gas	Ar, 12 l/min	Particles size	10 ÷ 45 μm
Pressure: primary/carrier	170 psi, 110 psi	Preheated powder	90 $^\circ\text{C}$

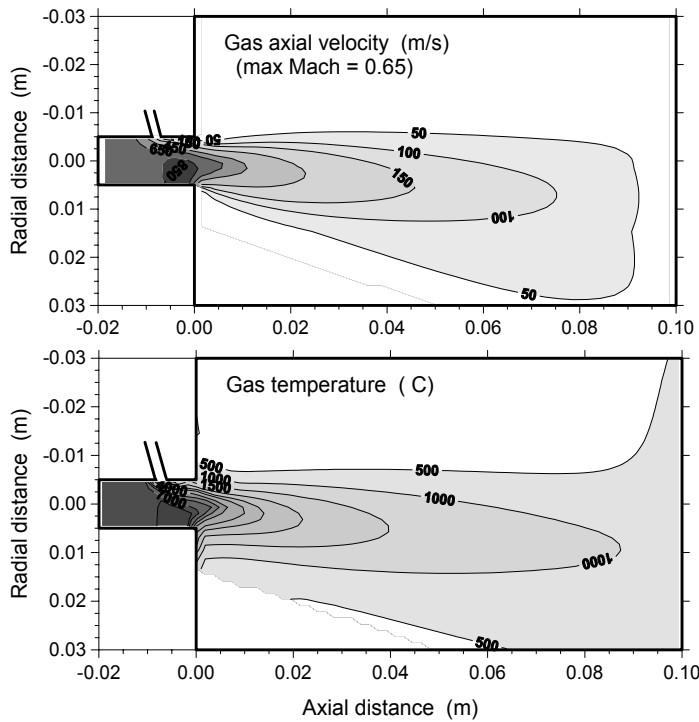


Figure 6. Gas velocity and temperature field.

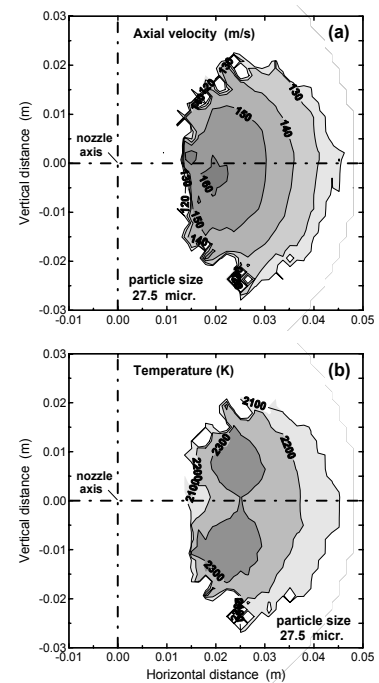


Figure 7. Impact conditions of particles: α) u_p , β) T_p

Using the numerical results for the particulate phase, the coating thickness produced after each traverse of the spraying gun (gun speed: 276 mm/s) can be calculated.

The material coating shows a normal distribution of the thickness in the cross-direction to the gun motion with a maximum thickness of 18 μm per pass (Figure 8). The above results are in a good agreement with the corresponding observations of CERECO (jet slope and spread, coating thickness and pattern).

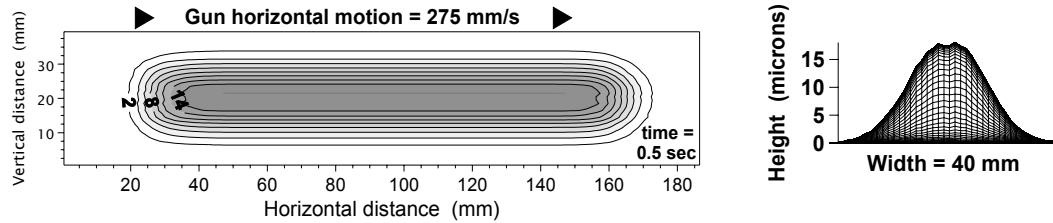


Figure 8. Coating width distribution on the surface, after one gun traverse.

3.3 Prediction of coating quality

The adjustment of the coefficients of the equations (5) and (6) has been based on the efficiency and porosity measurements of CERECO, shown in Table 3. Case 2 refers to a longer distance from the surface to be coated, case 3 to a lower speed and case 4 to a lower arc intensity, compared to the basic case 1.

Table 3. Experimental cases and comparison numerical results.

	Case 1	Case 2	Case 3	Case 4
Electrical intensity (A)	700	700	700	600
Volume (V)	85	85	85	85
Distance (mm)	100	110	100	100
Gun speed (m/s)	0.275	0.275	0.134	0.275
Porosity (%)	5.5	5.2	7.2	4.9
Efficiency (%)	52	46	70.5	49
Numerical results (coefficients' adjustment using cases 1 & 3)				
Porosity (%)	5.40	5.12	7.21	5.04
Efficiency (%)	51.9	48.0	70.8	48.5

In each of the above cases, after the convergence of the corresponding two-phase flow field, the trajectories of 110000 particles of size 10-45 μm are calculated, in order to produce the variables N_i and $D_{s,i}$ of equation (4). Next, the coated surface fraction P_c is produced by the spatial and time integration of (4) for the time period in which the gun makes one traverse (Figure 2).

The numerical results included in Table 3 are in a very good agreement with the measurements of cases 1 and 3, for which the coefficients of the model have been adjusted. In addition, the comparison of the other two cases is also satisfactory, verifying the correct behaviour of the model.

3.4 Parametric study

The computational model was also used in a parametric study of the influence of several spraying conditions of the CERECO gun, as the distance from the surface (80-120mm), the arc intensity (600-800 A) and the gun traverse speed (0.1-0.3 m/s) on the spraying efficiency and coating quality. Interesting conclusions have been drawn some of which are plotted in Figure 9. The spraying efficiency (powder usage) and quality (porosity) are competitive

parameters, i.e. improvement in quality decreases the efficiency and vice versa; the coating quality is improved reducing the arc intensity or increasing the spraying distance, but both these variations decrease the particles' impact velocity and impact temperature, hence they have a limit; the increase of the gun speed improves the coating quality but not the efficiency; the rate of these variations is decreased in high traversing speed.

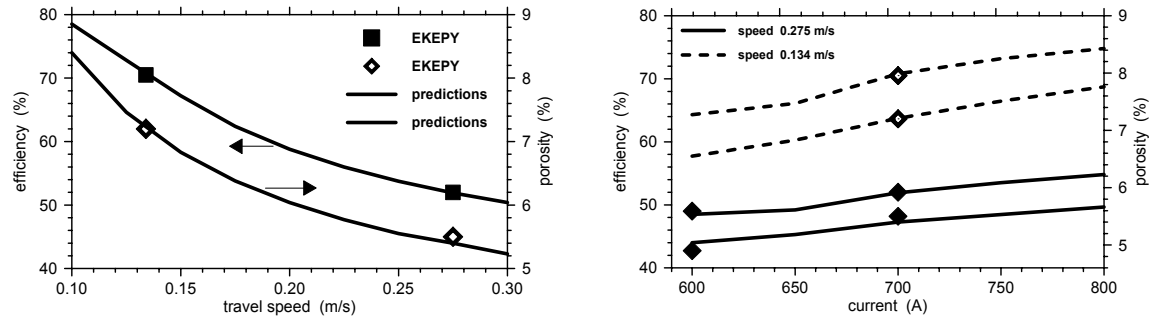


Figure 9. Effect of gun speed and arc intensity on the coating quality.

4. Conclusions

The developed model can simulate both qualitatively and quantitatively the physical parameters existing in the thermal spraying process of metal powder under ambient pressure. Therefore, it can be used for accounting the influence of several geometrical and operating parameters in order to optimize the thermal spraying process.

The code simulating the quality of the coating of a particular arrangement needs however basic experimental data in order to adjust its coefficients. The existence and the analysis of more measurements in corresponding arrangements could help in producing general expressions for these coefficients and also in introducing other more elaborated mechanisms of material coating and porous formation.

Acknowledgments: This study was supported by GGET, 97 EKBAN2-126 work.

References

- [1] Apelian D, Paliwal M, Smith R and Schilling W 1983 *Int. Metals Rev.* **28** (5) 271-294.
- [2] Jog M and Huang L 1996 *J. Heat Transfer* **118** 471-477.
- [3] Pfender E 1989 *Plasma in Chemistry and Processing* **9** (1) 1675-1945.
- [4] Madjeski J 1976 *Int. J. of Heat and Mass Transfer* **19** 1009-1013.
- [5] Trapaga G and Szekeley J 1991 *Metallurgical Transactions B* **22B** 901-914.
- [6] Liu H, Lavernia E and Rangel R 1993 *J. of Physics D: Applied Physics* **26** 1900-1908.
- [7] Anagnostopoulos J and Bergeles G 1992 *Int. J. of Heat and Fluid Flow* **13** (2) 141-150.
- [8] Sargianos N, Anagnostopoulos J and Bergeles G 1993 *Int. J. for Numerical Methods in Fluids* **16** 287-301.
- [9] Lee Y C 1984 *Modeling Work in Thermal Plasma Processing* Ph.D. Thesis Univ. of Minnesota, USA.
- [10] Anagnostopoulos J and Bergeles G 1999 *Metallurgical and Materials Transactions B* **30** (6) 1095-1105.